In vivo radioactive metabolite analysis for individualized medicine: A basic study of a new method of CYP activity assay using ^{123}I-IMP

Kodai Nishi [a,b], Asuka Mizutani [b], Naoto Shikano [c], Ken-ichi Fujita [d], Masato Kobayashi [b], Masahiro Ono [b,e], Ryuichi Nishii [f], Yasutuna Sasaki [d], Seigo Kinuya [g], Keiichi Kawai [b,h],*

[a] Department of Radioisotope Medicine, Atomic Bomb Disease institute, Nagasaki University, Nagasaki, Japan
[b] School of Health Science, College of Medical, Pharmaceutical and Health Sciences, Kanazawa University, Ishikawa, Japan
[c] Department of Radiological Sciences, Ibaraki Prefectural University of Health Science, Ibaraki, Japan
[d] Institute of Molecular Oncology, Showa University, Tokyo, Japan
[e] Research Center, Nihon Medi-Physics Co., Ltd., Chiba, Japan
[f] University of Miyazaki Hospital, Miyazaki, Japan
[g] School of Medical Sciences, College of Medical, Pharmaceutical and Health Sciences, Kanazawa University, Ishikawa, Japan
[h] Biomedical Imaging Research Center, University of Fukui, Fukui, Japan

ABSTRACT

Introduction: ^{123}I-N-isopropyl-p-iodoamphetamine (^{123}I-IMP) is metabolized and converted to ^{123}I-p-iodoamphetamine (^{123}I-PIA) by CYP2C19 in humans. Since variations in ^{123}I-PIA levels reflect variations in CYP2C19 activity, CYP2C19 activity can be estimated by quantitative analysis of ^{123}I-PIA levels. Thus, ^{123}I-IMP administration can provide diagnostic information not only regarding cerebral blood flow (rCBF) but also regarding metabolic function. The aim of the present study was to detect variations in CYP activity in mice using metabolite analysis.
Methods: Metabolism of ^{125}I-IMP in pooled homogenates of mouse liver (MLH) was analyzed by high-performance liquid chromatography (HPLC) in the presence or absence of NADPH. The amount of ^{125}I-PIA generated was calculated as the normalized peak area of the chromatogram. Inhibition of ^{125}I-IMP metabolism was evaluated using the inhibitor SKF-525A. A biodistribution study of ^{125}I-IMP was performed to determine the organ distribution of ^{125}I-IMP/^{125}I-IMP metabolites and the effect of SKF-525A. Variations in CYP activity *in vivo* were detected by administration of ^{123}I-IMP and/or SKF-525A to mice. The liver and the kidney were then excised, homogenized and analyzed using HPLC.
Results: ^{125}I-IMP was metabolized by MLH in the presence of NADPH, and the production of ^{125}I-PIA was inhibited by SKF-525A. SKF-525A did not greatly affect the biodistribution of ^{125}I-IMP/^{125}I-IMP metabolites *in vivo*. Both ^{123}I-IMP and ^{123}I-PIA were detected in organs of control mice. However, ^{123}I-PIA was not detected in the livers or kidneys of mice treated with SKF-525A.
Conclusions: CYP activity *in vivo* was inhibited by SKF-525A treatment. Variations in CYP activity could be detected in the blood, liver and kidney as changes in the peak area of ^{123}I-PIA.
Advances in knowledge and implications for patient care: ^{123}I-IMP metabolite analysis has the potential to provide beneficial information for prediction of the effect of medicines, in addition to its contribution to more accurate rCBF diagnosis that reflects individual CYP activity.

© 2014 Elsevier Inc. All rights reserved.

1. Introduction

The ideal radiopharmaceutical is generally not metabolized and does not undergo a structural change *in vivo*. Radiopharmaceuticals can be used for both tissue accumulation studies and/or for tissue metabolic studies. For the former study, the ideal radiopharmaceutical is generally not metabolized and does not undergo a structural change *in vivo*. For the latter study, the ideal radiopharmaceutical is only metabolized after its accumulation in the target tissue. An important feature of nuclear medicine images is that these images reflect biological functions. Radiopharmaceuticals that are administered to the body provide information regarding the biological functions that are involved in their accumulation, which vary according to the chemical structure of the radiopharmaceutical. If the structure of the radiopharmaceutical changes before it goes into the tissues, then the behavior of this modified radiopharmaceutical will differ from that of the administered parental radiopharmaceutical. Thus, nuclear medicine images obtained with such a radiopharmaceutical would not accurately reflect biological

function. However, some radiopharmaceuticals are known to be metabolized *in vivo* and such radiopharmaceuticals can provide important biological data [1]. In particular, [123]I-*N*-isopropyl-*p*-iodoamphetamine (^{123}I-IMP) is metabolized in stages and converted to [123]I-*p*-iodoamphetamine (^{123}I-PIA) [2].

Currently, ^{123}I-IMP is widely used in clinical practice to examine regional cerebral blood flow (rCBF) [3,4]. The input function of ^{123}I-IMP is calculated based on octanol–water partition coefficients because the lipophilic nature of the ^{123}I-IMP metabolites gradually decreases as ^{123}I-IMP is metabolized. However, ^{123}I-IMP can potentially provide not only rCBF data but also data regarding another important diagnostic parameter; CYP activity. Our research group has identified CYP2C19 as the enzyme that metabolizes *N*-isopropyl-*p*-iodoamphetamine (cold-IMP) and has shown using high-performance liquid chromatography (HPLC) that CYP2C19 converts cold-IMP to *p*-iodoamphetamine (cold-PIA) in pooled microsomes from human liver (HLM) [5].

CYP2C19 is one of the cytochrome P450 enzymes that are involved in the metabolism of medicines [6]. However, four phenotypes of the CYP2C19 gene are expressed; extensive metabolizer (EM), intermediate metabolizer (IM), poor metabolizer (PM), and ultra-rapid metabolizer (UM) [7]. In general, a PM has little ability to metabolize medicines, and therefore is susceptible to side effects of such medicines. Thus, if PM is the only, or the major CYP2C19 gene expressed, the subject is susceptible to side effects of normal doses of administered commonly-used medications.

It is therefore important to establish a method for measurement of the medicine-metabolizing capacity of individuals. Our research group focused on analysis of the metabolites of ^{123}I-IMP as a means of quantifying CYP2C19 activity in individuals. Since changes in ^{123}I-PIA production may reflect variations in CYP2C19 activity, it should be possible to determine CYP2C19 activity in individuals by quantitative analysis of their ^{123}I-PIA levels following ^{123}I-IMP administration.

In the present study, we aimed to detect variations in CYP activity in a living organism by performing metabolic experiments in mice. These data can be used as a basic study of ^{123}I-IMP metabolite analysis for individualized medicine.

2. Materials and methods

2.1. Materials

Reagent-grade chemicals (e.g. potassium dihydrogenphosphate, dipotassium hydorogenphosphate, disodium edetate dihydrate, 60% perchloric acid, p-chlorobenzoic acid, and acetonitrile) were purchased from Nacalai Tesque (Kyoto, Japan). B-NADP$^+$ and glucose-6-phosphate dehydrogenase were obtained from Oriental Yeast (Osaka, Japan). SKF-525A was obtained from Enzo Life Science (Zandhoven, Belgium). ^{125}I-IMP and ^{123}I-IMP were provided free by Nihon Medi-Physics (Chiba, Japan).

2.2. Preparation of pooled homogenates of mouse liver (MLH)

Animal studies were approved by the Animal Care Committee at Kanazawa University and were conducted in accordance with international standards for animal welfare and institutional guidelines.

Six male mice (ddY, 6 weeks old, Japan SLC, Tokyo, Japan) were euthanized with anesthesia using diethyl ether. The liver was then removed and weighed. After addition of Krebs–Ringer phosphate buffer (KRPB, pH 7.4) to the livers, the mixture was homogenized using an ultrasonic homogenizer. The protein content was quantified using the bicinchoninic acid method [8].

2.3. Metabolism of ^{125}I-IMP by MLH

NADPH-dependent metabolism of ^{125}I-IMP (370 kBq) by the pooled MLH samples was examined in an incubation mixture consisting of 100 mM sodium potassium phosphate buffer (pH 7.4), 50 μM EDTA disodium salt, and 250, 500, 1000 or 2000 μg protein/10 μL pooled MLH in a final volume of 250 μL, in the presence or absence of an NADPH-generating system (0.5 mM NADP$^+$, 5 mM MgCl$_2$, 5 mM glucose-6-phosphate, and 1 U/mL glucose-6-phosphate dehydrogenase). A mixture without MLH or NADPH was used as the control. The mixture was incubated at 37 °C for 20, 40 or 60 min. The reaction was stopped by adding 50 μL perchloric acid following which p-chlorobenzoic acid (20 μM, 30 μL) was added as an internal standard for ultraviolet (UV) detection. Subsequently, the mixture was centrifuged for 5 min at 18000 g, and 100 μL supernatant was analyzed using HPLC equipped with UV and gamma (γ)-ray detectors.

2.4. SKF-525A inhibition of ^{125}I-IMP metabolism by MLH

SKF-525A was used as a selective CYP inhibitor [9,10]. Inhibition of ^{125}I-IMP (370 kBq) metabolism by pooled MLH was examined in an incubation mixture consisting of 100 mM sodium potassium phosphate buffer (pH 7.4), SKF-525A (final concentration of 1, 5, 10 or 15 μM), 50 μM EDTA disodium salt and 1000 μg protein/10 μL MLH in a final volume of 250 μL, in the presence or absence of the NADPH-generating system.

The mixture was incubated at 37 °C for 20 min. The reaction was stopped by adding perchloric acid, following which 20 μM p-chlorobenzoic acid was added as the internal standard. Subsequently, these samples were centrifuged for 5 min at 18000 g, and 100 μL supernatant was analyzed using HPLC.

2.5. Biodistribution studies of ^{125}I-IMP in mice

These studies were performed to evaluate the effects of SKF-525A on the biodistribution of administered ^{125}I-IMP. Male mice (ddY, 6 weeks old) were pretreated with SKF-525A in saline solution (1.25 μM, 100 μL) or with saline alone (100 μL), and, after 3 min, ^{125}I-IMP (18.5 kBq, 100 μL) was administered via the tail vein. Mice were sacrificed at 2, 5, 10, 15 and 20 min after injection of ^{125}I-IMP by cervical dislocation under deep ether anesthesia, and blood and organs of interest were removed. Organs were weighed and their radioactivity was then determined using a scintillation counter. The ratio of radioactivity accumulated per injected dose (ID) per organ weight was determined after decay correction and is expressed as a percentage (%ID/g).

2.6. Metabolism of ^{123}I-IMP and its inhibition by SKF-525A in mice

Mice were pretreated with or without SKF-525A (1.25 μM, 100 μL) in saline solution, and, 3 min later, ^{123}I-IMP (7.4 MBq, 100 μL) was administered via the tail vein. Fifteen minutes after ^{123}I-IMP injection, mice were sacrificed by cervical dislocation under deep ether anesthesia. Blood was collected and deproteinized by adding 50 μL perchloric acid. Subsequently, the mixture was centrifuged for 5 min at 18000 g, and 100 μL supernatant was analyzed using HPLC. The liver and kidney were excised and weighed. After addition of KRPB to the liver and kidney, the mixture was homogenized using an ultrasonic homogenizer. The homogenates were deproteinized by adding perchloric acid, centrifuged for 5 min at 18000 g, and 100 μL supernatant was analyzed using HPLC.

2.7. HPLC analysis of [125]I- or ^{123}I-IMP

[125]I- or ^{123}I-IMP and p-chlorobenzoic acid were analyzed using an HPLC system consisting of a pump (model L-7100, Hitachi, Tokyo, Japan), a UV detector (model SPD-10A, SHIMADZU, Tokyo, Japan) and a γ-ray detector (model RLC-701, Hitachi-Aloka Medical, Japan) equipped with a 5C$_{18}$ AR-II column (4.6 × 250 mm; 5 μm, Nacalai Tesque). The mobile phase consisted of 60% (v/v) 20 mM potassium phosphate buffer (pH 3.0) and 40% acetonitrile. Signal intensity was expressed as voltage (V, or mV). The amount of [125]I- or ^{123}I-PIA was

evaluated as the normalized peak area (%). The normalized peak area of ^{125}I- or ^{123}I-PIA was defined as follows: Ratio of the peak area of ^{125}I- or ^{123}I-PIA to the total area of significant peaks.

2.8. Selection of radioactive isotope (RI)

^{125}I-IMP was used instead of ^{123}I-IMP for *in vitro* experiments and the biodistribution study because of its longer half-life. However, to detect radioactivity in the *in vivo* CYP activity assay using the HPLC system, it was necessary to have high levels of radioactivity in the homogenates of the excised organs. Unfortunately, the concentration of ^{125}I-IMP in the homogenates was too low for detection by this assay. Since the volume of ^{125}I-IMP solution that would contain the required radioactivity was too large to administer to mice, we therefore used ^{123}I-IMP for the *in vivo* CYP activity assay experiment.

2.9. Statistical analysis

All results represent the average of least three experiments and are expressed as the mean ± SD. Data were analyzed using Student's *t*-test, and $P < 0.05$ was considered statistically significant.

3. Results

^{125}I-IMP metabolism to ^{125}I-PIA in MLH was analyzed using HPLC. In *in vitro* experiments, the peaks of parental ^{125}I-IMP and the metabolite ^{125}I-PIA were detected in an incubation mixture containing an NADPH-generating system as shown in Fig. 1A. In contrast, only parental ^{125}I-IMP was detected in a reaction mixture in the absence of the NADPH-generating system (Fig. 1B). The normalized peak area of ^{125}I-PIA increased depending on the incubation time and the MLH concentration (Fig. 2). At each incubation time, the normalized peak area of ^{125}I-PIA was maximal at 1000 μg protein/sample, and was lower at 2000 μg protein/sample due to NADPH depletion.

In the metabolic inhibition experiment *in vitro*, ^{125}I-PIA production was reduced in a concentration-dependent manner following addition of the selective CYP inhibitor SKF-525A (Fig. 3). The normalized peak
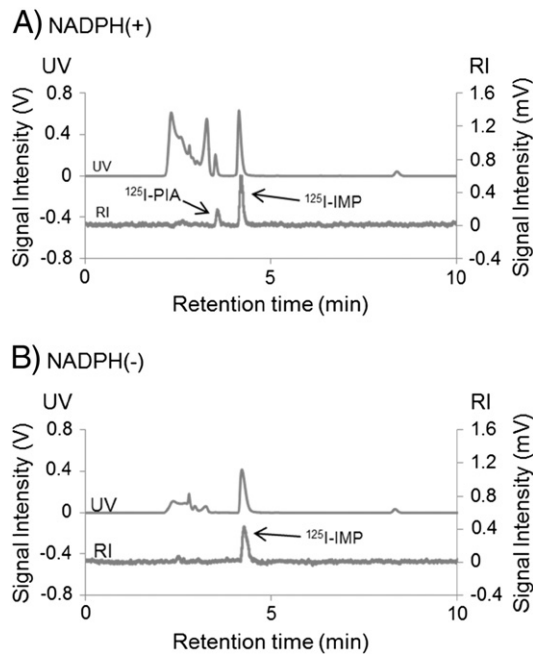
Fig. 1. Chromatograms of *in vitro* metabolite analyses. MLH (1000 μg protein/sample) was incubated in the presence (A) or absence (B) of NADPH for 60 min and then analyzed by HPLC. The peaks of parental ^{125}I-IMP and of ^{125}I-PIA are shown. ^{125}I-PIA was only detected in the presence of NADPH.
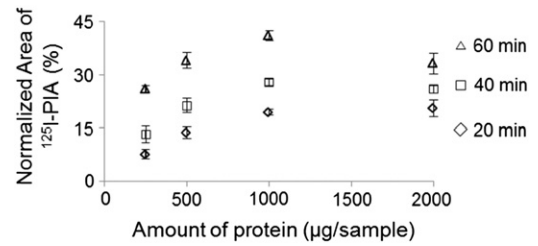
Fig. 2. Relationship between MLH protein concentration and the normalized peak area of ^{125}I-PIA at each incubation time *in vitro*. MLH at the indicated protein concentration was incubated with ^{125}I-IMP for the indicated times in the presence of NADPH. Samples were analyzed by HPLC and the normalized peak area of ^{125}I-PIA was calculated. Error bars represent the mean ± SD.

area of ^{125}I-PIA was reduced by approximately 50% in the presence of 10 μM SKF-525A.

Tables 1A and 1B show the *in vivo* biodistribution of ^{125}I (^{125}I-IMP plus ^{125}I-PIA) in each mouse organ as a percentage of the injection dose/g tissue (%ID/g) or/mL blood (%ID/mL) in the absence (1A) or presence (1B) of SKF-525A. In both the control and the SKF-525A group, ^{125}I (^{125}I-IMP plus ^{125}I-PIA) showed higher accumulation in the kidney compared to other organs except for the lung, and the level of radioactivity in the blood was very low. In addition, no radioactivity was detected in the urine. Fig. 4 shows the *in vivo* data for blood, liver and kidney from Tables 1A and 1B in graph form and compares the effect of SKF-525A on accumulated radioactivity. There was no significant difference in the radioactive blood levels (A), or in the accumulated radioactivity levels in the liver (B) between the groups with or without SKF-525A. However, in the kidney (C), the accumulated level of ^{125}I-IMP plus ^{125}I-PIA at 5 min was higher in the SKF-525A group than in the control group ($P < 0.05$). These results indicate slightly faster distribution of ^{125}I-IMP plus ^{125}I-PIA to the kidney following co-administration of SKF-525A.

In HPLC analysis of the blood of mice administered ^{123}I-IMP, peaks of parental ^{123}I-IMP and the metabolite ^{123}I-PIA were detected in both the control and the SKF-525A groups. However, the normalized peak area of ^{123}I-PIA was markedly and significantly reduced compared with the control group due to the SKF-525A loading. Moreover, whereas peaks of both ^{123}I-IMP and ^{123}I-PIA were detected in organ homogenates prepared from control mice, only a peak of parental ^{123}I-IMP was detected in organ homogenates prepared from mice loaded with SKF-525A (Table 2).

4. Discussion

Considerable individual differences exist in the pharmacokinetics of humans. In most cases, the differences result from individual differences
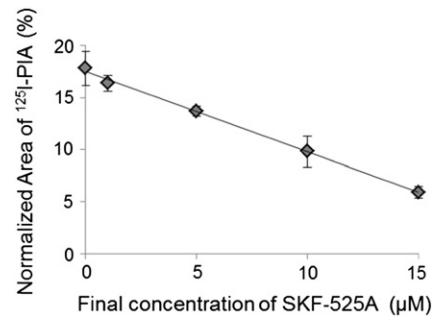
Fig. 3. Effect of SKF-525A concentration on ^{125}I-PIA generation *in vitro*. MLH (1000 μg protein/sample) was incubated with ^{125}I-IMP for 20 min in the presence of the indicated concentration of SKF-525A. The normalized peak area of ^{125}I-PIA was determined using HPLC. Error bars represent the mean ± SD. The normalized peak area of ^{125}I-PIA decreased with increasing SKF-525A concentration.

Table 1A
Biodistribution of ^{125}I-IMP and its metabolites in mice not pretreated with SKF-525A.

Organ	Time after ^{125}I-IMP injection				
	2 min	5 min	10 min	15 min	20 min
Blood	0.67 ± 0.07	0.64 ± 0.16	0.74 ± 0.11	0.74 ± 0.12	0.76 ± 0.04
Brain	5.46 ± 0.48	5.36 ± 0.96	7.29 ± 1.96	6.42 ± 0.09	6.57 ± 0.26
Lung	21.79 ± 5.60	16.82 ± 5.14	17.70 ± 4.65	13.82 ± 1.26	13.14 ± 1.79
Heart	5.51 ± 0.85	4.06 ± 0.88	4.10 ± 0.98	3.93 ± 0.68	3.33 ± 0.02
Liver	2.68 ± 0.29	3.44 ± 0.79	4.97 ± 0.43	4.67 ± 0.08	4.79 ± 0.19
Pancreas	4.40 ± 1.61	6.85 ± 1.58	10.35 ± 2.22	11.16 ± 0.90	10.63 ± 0.24
Spleen	2.49 ± 0.51	3.85 ± 0.63	8.15 ± 0.87	4.54 ± 1.62	6.66 ± 0.16
Stomach	2.70 ± 0.48	3.42 ± 0.86	7.13 ± 2.10	7.05 ± 0.03	8.35 ± 1.88
Kidney	7.92 ± 1.08	9.43 ± 1.25	11.87 ± 1.92	12.04 ± 0.54	10.33 ± 0.83
Intestine	1.98 ± 0.15	2.13 ± 0.40	3.09 ± 0.38	2.75 ± 0.04	2.80 ± 0.19
Muscle	2.77 ± 0.54	2.27 ± 0.19	2.19 ± 0.13	1.78 ± 0.15	1.90 ± 0.15
Urine	N.D.	N.D.	N.D.	N.D.	N.D.

%ID/g was calculated with the following formula: $100 \times$ (cpm of organ/injected dose)/organ weight. N.D.: Not detected.

in the activity of drug-metabolizing enzymes as typified by CYP. Genetic polymorphisms are cited as the main factors responsible for individual differences in the activity of drug-metabolizing enzymes [11,12]. Individuals with very low or very high metabolic capacities exist due to genetic polymorphisms in CYP, and are described as PM and EM respectively [13,14]. Currently, such individual differences at the genetic level are distinguished by genetic analysis. However, genetic analysis cannot determine individual metabolic capacity at a particular point of time, which involves a variety of factors such as concomitant ingestion of different medicines, alcohol intake and deterioration in liver function due to aging. On the other hand, our method based on metabolite analysis can measure an individual's metabolic capability that reflects all of the factors described above. As previously indicated, to date ^{123}I-IMP has only been used to examine rCBF. However, based on our data, ^{123}I-IMP will be able to provide diagnostic information regarding metabolic function. On a relevant note, it will also be possible to accurately calculate input function by measuring the amount of an ^{123}I-IMP metabolite because the ratio of lipophilic metabolites that contaminate the octanol fraction will change according to the CYP activity of the individual patient. Thus, the present study provides an important basis for accurate assessment of input function and for establishment of an index that can be used to determine the dose of medicine to be prescribed for individuals. In brief, competition with ^{123}I-IMP can be used for dose determination of medicines that are non-radioactive and are substrates of CYP2C19, such as imipramine, clomipramine, omeprazole and cimetidine. These non-radioactive medicines inhibit metabolism of ^{123}I-IMP in a similar manner to SKF-525A.

In our previous study with HLM, cold-IMP was metabolized by CYP2C19 to cold-PIA [5]. However, IMP-metabolizing enzymes in mice

have not been identified, and important species differences are present between humans and mice. In addition, the number of molecules of [125]I- or ^{123}I-IMP that are accumulated in HLM or in organs after in vivo administration is very low. For these reasons, it was necessary to detect [125]I- or ^{123}I-IMP, as well as cold-IMP, using an analytical method such as HPLC.

CYPs are drug-metabolizing enzymes that act when NADPH is present as an energy source [15]. In *in vitro* experiments, ^{125}I-IMP and ^{125}I-PIA were detected with high sensitivity using HPLC, and we confirmed that ^{125}I-IMP was metabolized and converted to ^{125}I-PIA only in the presence of NADPH. In addition, the normalized area of the ^{125}I-PIA peak increased in a manner that was dependent on the protein concentration of MLH and on the incubation time (Fig. 2). We therefore concluded that the metabolism of ^{125}I-IMP was due to an enzymatic reaction. Based on these results, the protein concentration and incubation time were set at 1000 μg/sample and 20 min respectively, because a sufficient normalized peak area was obtained under these conditions that permitted evaluation of changes in the amount of ^{125}I-PIA.

The aim of the in vitro experiments of metabolic inhibition was to confirm that IMP is metabolized by mouse CYP. Since it is unknown which CYP family metabolizes ^{125}I-IMP in mice, we used SKF-525A as a CYP inhibitor, because SKF-525A inhibits the function of CYP regardless of the family or subfamily classification of CYP. The normalized area of the ^{125}I-PIA peak was reduced in an SKF-525A concentration-dependent manner (Fig. 3). Based on these results, we inferred that ^{125}I-IMP was metabolized by CYP in mice as well as in humans.

In the biodistribution study, ^{125}I-PIA cannot be distinguished from ^{125}I-IMP, because they both contain the same radionuclide; [125]I. Therefore this study evaluated the overall biodistribution of ^{125}I-IMP

Table 1B
Biodistribution of ^{125}I-IMP and its metabolites in mice pretreated with SKF-525A.

Organ	Time after ^{125}I-IMP injection				
	2 min	5 min	10 min	15 min	20 min
Blood	0.87 ± 0.36	0.85 ± 0.03	0.91 ± 0.18	0.80 ± 0.29	0.81 ± 0.12
Brain	5.95 ± 2.22	6.83 ± 0.21	7.52 ± 0.98	6.96 ± 2.27	7.31 ± 0.59
Lung	17.88 ± 7.35	16.11 ± 2.11	18.91 ± 4.73	17.52 ± 5.53	16.32 ± 3.47
Heart	5.32 ± 2.28	5.29 ± 0.67	5.44 ± 0.17	4.38 ± 1.54	4.42 ± 0.30
Liver	3.35 ± 0.57	4.53 ± 0.10	5.85 ± 1.40	5.08 ± 1.25	4.76 ± 0.12
Pancreas	6.89 ± 3.24	8.46 ± 1.37	9.87 ± 0.59	7.63 ± 3.71	9.87 ± 0.63
Spleen	4.60 ± 1.84	5.83 ± 0.73	6.64 ± 0.75	6.80 ± 0.94	7.65 ± 0.52
Stomach	3.68 ± 1.66	4.81 ± 1.32	7.67 ± 0.69	9.04 ± 3.63	9.24 ± 3.38
Kidney	10.11 ± 2.46	11.90 ± 0.12	13.46 ± 1.52	12.01 ± 1.15	10.89 ± 1.10
Intestine	2.09 ± 0.24	2.49 ± 0.15	3.24 ± 0.34	2.72 ± 0.71	2.52 ± 0.22
Muscle	2.27 ± 0.67	2.83 ± 0.32	2.54 ± 0.25	1.99 ± 0.89	2.24 ± 0.19
Urine	N.D.	N.D.	N.D.	N.D.	N.D.

%ID/g was calculated with the following formula: $100 \times$ (cpm of organ/injected dose)/organ weight. N.D.: Not detected.
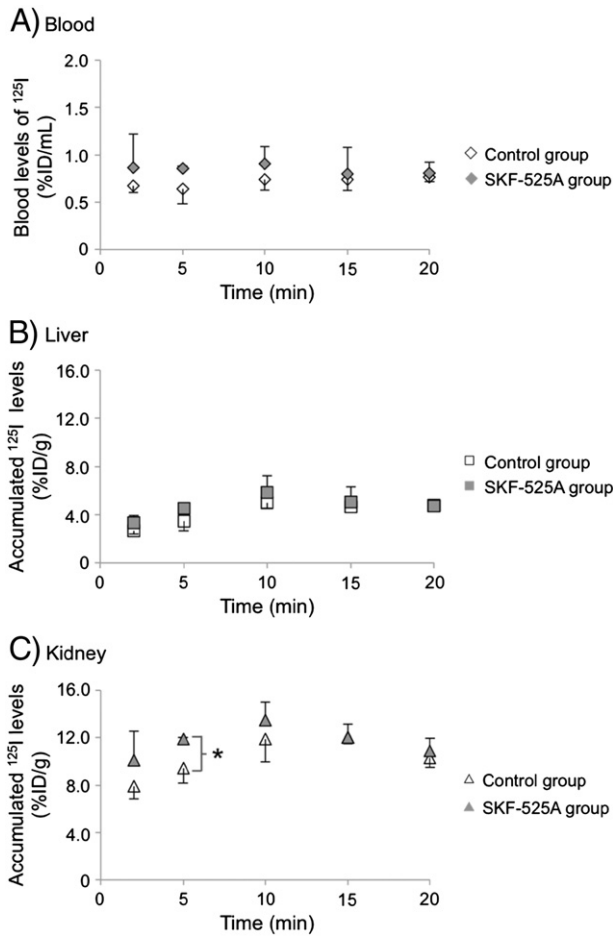
Fig. 4. Graphic analysis of the *in vivo* effect of SKF-525A on the accumulation of ^{125}I-IMP and its metabolites in specific organs. Radioactive (^{125}I) levels in the blood (A), liver (B) and kidney (C) of mice pretreated with SKF-525A or saline for 3 min prior to injection of ^{125}I-IMP, as indicated in Tables 1A and 1B, are shown in graph form. ID; injected dose. Error bars represent the mean $\pm$ SD. *: $P < 0.05$ compared with control group. Little difference was noted between the control and SKF-525A groups.

including ^{125}I-IMP metabolites. This biodistribution study indicated a significant difference in the accumulation of ^{125}I-IMP/^{125}I-IMP metabolites in the kidney at 5 min between the control and the SKF-525A group. However, no significant difference was found in the accumulation of ^{125}I-IMP at other times or in other tissues between the two groups. Thus, we observed few significant alterations in the pharmacokinetics of ^{125}I-IMP due to preloading of SKF-525A. In both the control and SKF-525A groups, radioactivity in organs had almost reached equilibrium 15 min after administration of ^{125}I-IMP, indicating that tissue migration of ^{125}I-IMP had reached a steady state at this time point. As shown in Table 2, following preloading of SKF-525A, the peak of ^{123}I-PIA disappeared in the liver and kidney and the normalized peak area of ^{123}I-PIA was significantly reduced in the blood. We considered that these decreases in ^{123}I-PIA levels were caused by decreased CYP activity, and not by administration of SKF-525A because the radioactivity in other organs was not significantly altered (Tables 1A and 1B and Fig. 4).

Table 2
Effect of SKF-525A on ^{123}I-PIA levels in organs of ^{123}I-IMP-treated mice.

Organ	Control group	SKF-525A group
Blood	25.78 $\pm$ 1.74	15.13 $\pm$ 1.10
Kidney	14.38 $\pm$ 7.31	N.D.
Liver	25.17 $\pm$ 7.61	N.D.

The normalized area of the ^{123}I-PIA peak in HPLC analysis is shown. N.D.: Not detectable.

In general, careful consideration is necessary in discussion of the metabolism of medicines administered at different concentrations, because it is known that the velocity of metabolic enzymatic reactions depends on the concentration of the substrate, and, furthermore, that metabolic enzymes other than the CYP family are present. However, when the focus is on main and important one enzyme and its labeled substrate, it is possible to discuss the metabolism of the labeled substrate that is administered at tracer concentrations based on the premise that the species and function of the enzymes that metabolize this substrate do not change in the presence of a tracer concentration of the substrate. An example of such a study is the microdose study reported by Tozuka et al [16]. The fact that there is no pharmacological change in *in vivo* conditions due to the presence of a tracer concentration of the substrate is an advantage in this kind of study. In the present study, ^{123}I-IMP administration does not exert a pharmacological effect because ^{123}I-IMP is present in trace amounts. However, the administered ^{123}I-IMP would accurately reflect individual metabolic function.

Although the present experiments were performed using mice, we consider that the metabolic rate of ^{123}I-IMP will similarly fluctuate depending on CYP activity in humans.

In humans, a medicine that is a substrate for CYP2C19 would behave as a CYP2C19 inhibitor instead of SKF-525A. Subsequent ^{123}I-IMP metabolite analysis would then indicate variation in CYP2C19 activity due to ingestion of the medicine.

In addition, the only radiopharmaceutical that can currently be used for CYP activity-measurement methods that are based on metabolic changes is ^{123}I-IMP. This is because radiopharmaceuticals used in this method must meet the following conditions: a metabolizing enzyme must have been identified, its metabolites must also be radioactive, and detection and separation from the parental substance must be easy. This method of estimation of CYP activity using ^{123}I-IMP metabolite analysis has the potential to contribute to more accurate functional diagnosis that reflects individual metabolic function, and to the establishment of an index for determination of the correct dose of medicine to be administered in humans. Therefore, this method will lead to the establishment of individualized medicine.

5. Conclusion

Our aim was to detect CYP activity *in vivo* by quantitative analysis of ^{123}I-IMP metabolites. In the present study, we have demonstrated the following: First, ^{123}I-IMP and ^{123}I-PIA in HMLC are detectable using HPLC. Second, the normalized peak area of ^{123}I-PIA decreased due to reduction of CYP activity caused by SKF-525A treatment. Finally, variations in CYP activity *in vivo* were detected in the blood, liver, and kidney of mice as changes in the normalized area of the ^{123}I-PIA HPLC peak.

For clinical application, it is necessary that ^{123}I-PIA can be detected in samples such as blood or urine that can be collected in a minimally invasive manner, instead of in liver or kidney. In addition, it will be necessary to find a simpler method of analysis, such as thin-layer chromatography, instead of HPLC. However, we confidently conclude that ^{123}I-IMP metabolite analysis can be used to detect variations in CYP activity *in vivo*. Consequently, metabolite analysis of ^{123}I-IMP can potentially be used in a clinical setting as a method for rCBF analysis that reflects metabolic function and estimates the metabolic capacity of patients.

References

[1] Cumming P, Yokoi F, Chen A, Deep P, Dagher A, Reutens D, et al. Pharmacokinetics of radiotracers in human plasma during positron emission tomography. Synapse 1999; 34:124–34.

[2] Baldwin RM, Wu JL. In vivo chemistry of iofetamine HCl iodine-123 (IMP). J Nucl Med 1988;29:122–4.

[3] Cohen MB, Graham LS, Yamada LS. [123I]iodoamphetamine SPECT imaging. Int J Radiat Appl Instrum A 1986;37:749–63.

[4] Mimura H, Sone T, Takahashi Y, Yoshioka K, Murase K, Matsuda H, et al. Measurement of regional cerebral blood flow with 123I-IMP using one-point venous blood sampling and causality analysis: evaluation by comparison with conventional continuous arterial blood sampling. Ann Nucl Med 2006;20:589–95.

[5] Fujita K, Sugiyama M, Akiyama Y, Hioki K, Kunishima M, Nishi K, et al. N-Isopropyl-p-iodoamphetamine hydrochloride is predominantly metabolized by CYP2C19. Drug Metab Dispos 2012;40:843–6.

[6] Daly AK. Pharmacogenetics of the major polymorphic metabolizing enzymes. Fundam Clin Pharmacol 2003;17:27–41.

[7] Saeed LH, Mayet AY. Genotype-phenotype analysis of CYP2C19 in healthy Saudi individuals and its potential clinical implication in drug therapy. Int J Med Sci 2013;10:1497–502.

[8] Smith PK, Krohn RI, Hermanson GT, Mallia AK, Gartner FH, Provenzano MD, et al. Measurement of protein using bicinchoninic acid. Anal Biochem 1985;150:76–85.

[9] Kauser K, Clark JE, Masters BS, de Montellano PR Ortiz, Ma YH, Harder DR, et al. Inhibitors of cytochrome P-450 attenuate the myogenic response of dog renal arcuate arteries. Circ Res 1991;68:1154–63.

[10] Nunoya K, Yokoi Y, Kimura K, Kodama T, Funayama M, Inoue K, et al. (+)-cis-3,5-dimethyl-2-(3-pyridyl) thiazolidin-4-one hydrochloride (SM-12502) as a novel substrate for cytochrome P450 2A6 in human liver microsomes. J Pharmacol Exp Ther 1996;277:768–74.

[11] van der Weide J, Steijns LS. Cytochrome P450 enzyme system: genetic polymorphisms and impact on clinical pharmacology. Ann Clin Biochem 1999;36(Pt 6): 722–9.

[12] Singh D, Kashyap A, Pandey RV, Saini KS. Novel advances in cytochrome P450 research. Drug Discov Today 2011;16:793–9.

[13] Alonso-Navarro H, Jimenez-Jimenez FJ, Garcia-Agundez JA. The role of CYP2C19 polymorphism in the development of adverse effects to drugs and the risk for diseases. Med Clin 2006;126:697–706.

[14] Wijnen PA, Op den Buijsch RA, Drent M, Kuijpers PM, Neef C, Bast A, et al. Review article: the prevalence and clinical relevance of cytochrome P450 polymorphisms. Aliment Pharmacol Ther 2007;26(Suppl. 2):211–9.

[15] Reed JR, Backes WL. Formation of P450.P450 complexes and their effect on P450 function. Pharmacol Ther 2012;133:299–310.

[16] Tozuka Z, Kusuhara H, Nozawa K, Hamabe Y, Ikushima I, Ikeda T, et al. Microdose study of ^{14}C-acetaminophen with accelerator mass spectrometry to examine pharmacokinetics of parent drug and metabolites in healthy subjects. Clin Pharmacol Ther 2010;88:824–30.